NENE 2020 September 7 - 10 PORTOROŽ SLOVENIA
29th International Conference Nuclear Energy for New Europe

Processing of Thermal-hydraulic Approximations in the GFR 2400 Fast Reactor Design

Filip Osuský
Slovak University of Technology in Bratislava, Faculty of Electrical Engineering and Information Technology, Institute of Nuclear and Physical Engineering,
Ilkovičova 3
812 19, Bratislava, Slovakia
filip.osusky@stuba.sk

Branislav Vrban, Štefan Čerba, Jakub Lüley, Vladimír Nečas
Slovak University of Technology in Bratislava, Faculty of Electrical Engineering and Information Technology, Institute of Nuclear and Physical Engineering,
Ilkovičova 3
812 19, Bratislava, Slovakia
branislav.vrban@stuba.sk, stefan.cerba@stuba.sk, jakub.luley@stuba.sk, vladimir.necas@stuba.sk

ABSTRACT

The paper investigates the influence of the used thermal-hydraulic approximations in the coupled calculations of Gas-cooled Fast Reactor design (hereby GFR 2400). The NESTLE code is used as coupled simulation tool and solves multigroup neutron diffusion equation by finite difference method that is internally coupled with thermal-hydraulic sub-channel code. The in-house developed code referred as TEMPIN is used to prepare the thermal-hydraulic data for GFR 2400 design. The TEMPIN code solves steady state heat balance equation with flowing coolant in triangular lattice cell together with temperature dependent thermal-hydraulic properties of the fuel, cladding and coolant. Based on calculated fuel bundle temperature distributions by the TEMPIN code, the thermal-hydraulic approximations suitable for the NESTLE code are processed. The results of the analyses are compared with the previous study utilizing the FLUENT code (from ANSYS code package system) for processing of thermal-hydraulic approximations. Changes in neutronic and thermal-hydraulic distributions are described and visualized in the paper.

1 INTRODUCTION

Transient coupled simulation codes are widely used to provide sufficient information about the neutronic and thermal-hydraulic behaviour of new reactor designs during the licensing processes. The deterministic coupled codes such as NESTLE [1] or PARCS [2] are used for this purpose and are accepted by the regulatory bodies within European Union [3]. For the accurate calculation performance of these codes, the appropriate neutronic and thermal-hydraulic approximations have to be prepared. The processing of the neutronic macroscopic cross-section library can be carried out by the TRITON sequence which is included within the SCALE code package system [4]. By the TRITON sequence, it is possible to prepare problem specific, homogenized, energy group collapsed neutronic library for different operational states of the nuclear system. The problem may be encountered when the library is processed for the fast reactor systems by the utilization of standard procedures proposed by TRITON primer [5]. Significant deviations of reaction rates between the TRITON 2D and full-core 3D model can

occur in the case of GFR 2400. The methodology and procedures of the macroscopic cross-section library processing for GFR 2400, made by the team at Slovak University of Technology (STU), was shown in previous works [6] and [7]. In the case of the GFR 2400, the issue arises also from the processing of thermal-hydraulic approximations. The main reason is a lack of thermal-hydraulic benchmarks that are sufficiently representative for the GFR 2400 design. Therefore, thermal-hydraulic approximations of GFR 2400 prepared in this study are defined based on a literature survey in combination with the utilization of in-house developed code referred as TEMPIN. TEMPIN code solves steady state heat balance equation within the fuel pin (fuel, helium gap and cladding) including the thermal expansion of the fuel and the cladding together with the heat transfer to the flowing helium around the pins within the fuel bundle. Simulations can be performed on 2D domain that represents one fuel bundle and the results of radial temperature distribution serves as the steppingstone in the process of the thermal-hydraulic approximations preparation suitable for the NESTLE code.

In next section, the brief overview of the GFR 2400 design is presented. Subsequently, the methodology of thermal-hydraulic approximation processing is elaborated for the FLUENT CFD code [8] and for the TEMPIN code. Afterwards, the results of TEMPIN calculation are compared with the results obtained by the FLUENT code together with the application of the prepared approximations in the NESTLE coupled code.

2 GFR 2400 OVERVIEW

The design of the GFR 2400 consists from two separate fuel regions (Fig. 1-a). The fuel material is (U-Pu)C with additional americium content. Inner core region consists of 264 fuel assemblies with volumetric enrichment of PuC 14.12 % and outer core region accommodates 252 fuel assemblies with enrichment of PuC 17.65 %. Together 217 fuel pins are located in one fuel assembly (Fig. 1-b) with the lattice pitch 1.157 cm. The dimensions and material composition of the fuel pin are shown in Fig. 2. In this study, 18 control safety devices (CSD) are used for the reactivity control and 13 diverse safety devices (DSD) are placed in the upper parking position. Neutron trap (NT) passive safety system consist of 36 assemblies located above the core during normal operation. The passive actuation mechanism of the NT is Curie point latch with ALNICO material. The Curie point temperature of ALNICO is 800 °C at witch this material looses its magnetic properties. Thermal power of the GFR 2400 design is 2 400 MW and helium coolant is pressurized in primary circuit to 7 MPa. The coolant mass flow rate is 1 213 $kg.s^{-1}$ in whole core and the inlet temperature of the coolant is 400 °C. More details about the GFR 2400 design can be found in former analyses [6] and [9].

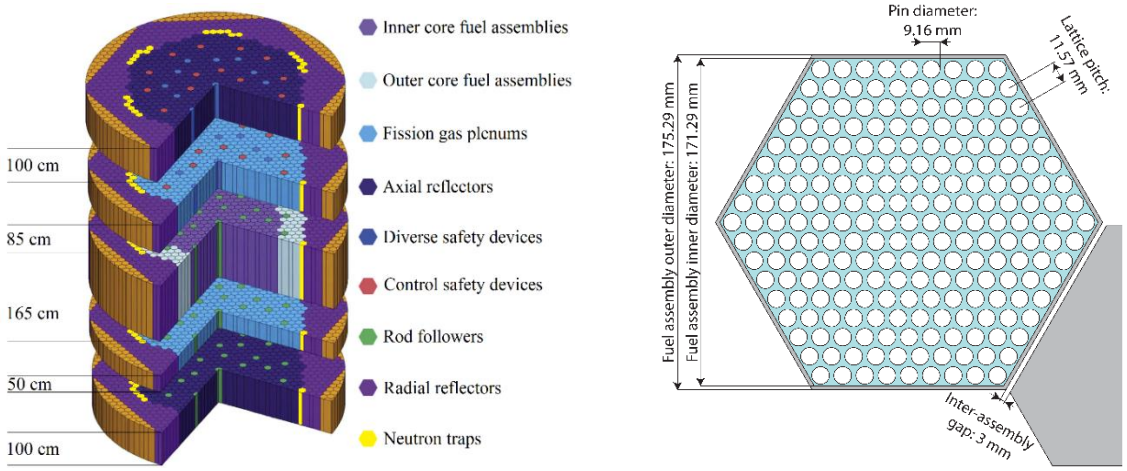

a) View of GFR 2400 core b) Design of FA

Figure 1: Cross sectional view of the GFR 2400 core and the fuel assembly [10]

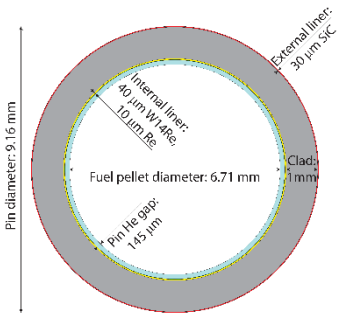

Figure 2: Cross sectional view of the fuel pin [10]

3 METHODOLOGY

3.1 FLUENT calculation procedures

Simplified model of the fuel pin was used for the calculation with the FLUENT code. To speed up whole calculation process, the one-sixth symmetry (of the hexagon) was considered and the used geometry is shown in Fig. 3. Temperature dependant thermal-hydraulic material properties were modeled in this simulation with compressible solver. The standard *k*-ε turbulent model was used together with standard wall functions. Besides, simple scheme was used in pressure-velocity coupling with default setup of spatial discretization in the FLUENT code. Symmetrical boundary condition was used in radial direction of the fuel pin. Inlet velocity condition was used at the bottom of the fuel pin and the coolant flow was set to 98.2 $m.s^{-1}$. The pressure outlet boundary condition was set to maintain 7 MPa pressure within the fuel pin. Base on the given thermal-hydraulic conditions and geometry, the Reynolds number was estimated by the FLUENT code on the level 434 (estimated flow is laminar). The constant heat generation term was used in the fuel region. To improve the simulation convergence rate, W14Re inner fuel pin cladding was homogenized together with SiC/SiC_f cladding. This simplification did not influence the calculation process significantly due to the fact that the thickness of that inner cladding liner is 50 µm and W14Re material is characterized by relatively high thermal conductivity [11]. More about the thermal-hydraulic properties of particular material mixes can be found in [7] and [9].

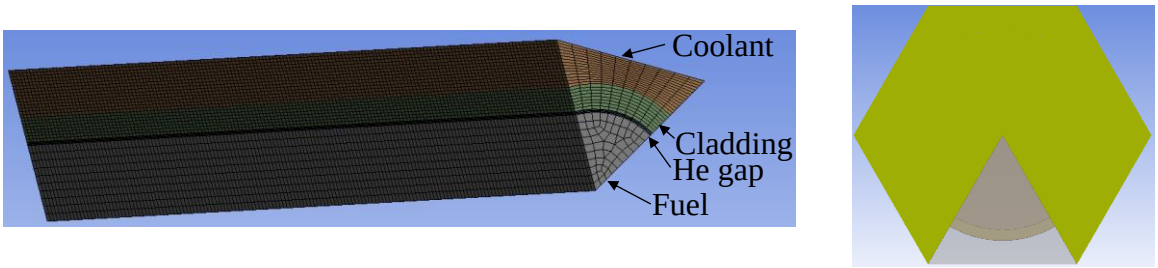

Figure 3: Geometry model used during FLUENT calculation including the mesh

3.2 TEMPIN calculation procedures

The approach adopted in the TEMPIN code is based on the analytical solution of the steady state heat balance equation, where the heat source is normalized by a rod linear power. The general fuel region heat balanced equation is expressed by Eq. (1).

$$\nabla\left(\lambda_f(T)\nabla T\right) + q_v = 0, \tag{1}$$

where λ_f represents the thermal conductivity of the fuel and q_v stands for the volumetric heat generation. Based on the radial neutron flux distribution (Eq. (2)) the heat generation term is reshaped by the constant χ.

$$\varphi(r) = \varphi_P \frac{I_0\left(\frac{\Sigma_a}{D} r\right)}{I_0\left(\frac{\Sigma_a}{D} r_f\right)} = \varphi_P \frac{I_0\left(\frac{1}{L^2} r\right)}{I_0\left(\frac{1}{L^2} r_f\right)} = \varphi_P \frac{I_0(\chi r)}{I_0(\chi r_f)}, \tag{2}$$

where φ is the neutron flux density, Σ_a stands for the absorption macroscopic cross-section, D represents the diffusion coefficient, L is the diffusion length and r_f stands for the fuel radius. The TRITON sequence is used for the determination of Σ_a and D constants. After integration of thermal conductivities by Simpson's rule, the temperature across the pin at location r can be numerically determined from the Eq. (3). This equation is applicable for the solid fuel pellet without a central hole.

$$\vartheta(T) - \vartheta_{FP} = \frac{2q_H[I_0(\chi r_f) - I_0(\chi r)]}{\chi r_f I_1(\chi r_f)}, \tag{3}$$

where $\vartheta(T)$ represents integral thermal conductivity of the fuel at the temperature T, ϑ_{FP} is the integral thermal conductivity at the fuel surface temperature and q_H stands for the linear heat generation. The cladding temperature distribution is expressed by the Fourier's law in Eq. (4).

$$q_H = -2\pi r \lambda_c \, {}^{dT}/_{dr}, \tag{4}$$

where λ_c is the thermal conductivity of the cladding. Based on the concept of integral conductivities, the cladding temperature can be expressed by the Eq. (5).

$$\vartheta(T) - \vartheta_{CP} = \frac{2q_H}{2\pi r} ln\left(\frac{r_{c_{out}}}{r}\right), \tag{5}$$

where ϑ_{CP} is the integral thermal conductivity for the temperature achieved at the outer cladding radius and $r_{c_{out}}$ is outer cladding radius. Dimensional changes of the gap due to the temperature evolution are also taken into account and the temperature increment within the gap is expressed only by thermal conduction term (Eq. (6)). Effect of radiation heat transfer was not considered and based on [12], this simplification should lead for underestimating of the maximal fuel temperature approximately 2 °C.

$$\Delta T_{Gap} = 2\pi r_f \alpha, \tag{6}$$

where empirical term α represents thermal conductivity properties of the gap at the given pressure including Knudsen's permeability correction. More about the TEMPIN code numerical solution can be found in [13]. The heat transfer from the cladding surface to the coolant is determined by the Newton`s law (Eq. (7)).

$$T_{CP} = \frac{q_H}{h_{CO} 2\pi r_{c_{out}}} + T_{CO}, \tag{7}$$

where T_{CP} represents outer cladding temperature, T_{CO} coolant reference temperature and constant h_{CO} stands for the heat transfer coefficient expressed by the Eq. (8).

$$h_{CO} = \frac{\lambda_{CO}}{d_h} Nu, \tag{8}$$

where λ_{CO} is thermal conductivity of the coolant, d_h represents hydraulic diameter of the fuel assembly and Nu stands for the Nusselt number. Based on the study [14], standard Dittus and Boelter expression can be applied for the modelling of the heat transfer properties of helium. Calculations presented in this study were carried out only for fresh fuel pins of GFR 2400. The used material properties for the thermal-hydraulic simulations can be found in the former analysis [6], [7] and [9].

3.3 NESTLE calculation procedures

The prepared thermal-hydraulic approximations (made by the FLUENT and TEMPIN codes) were implemented in the thermal-hydraulic model of GFR 2400 within the NESTLE code. The differences between these two approaches were observed for one steady state coupled simulation and for one transient coupled simulation. Rapid withdrawal of one control rod assembly from the ring located near the core center during nominal power operation was considered as the transient scenario. The withdrawal time was set to 0.2 s and the coolant outlet temperature evolution was observed to determine the actuation of the particular neutron trap (NT) assembly in the system. The actuation temperature of the NT assembly is 800 °C and the actuation mechanism is in the form of Curie point latch. The insertion time of one NT was set to 2 s. More about the transient simulation and about the processing of macroscopic cross-section library for the NESTLE code can be found in [6] and [7].

4 RESULTS AND DISCUSSION

The results of temperature profile at different radial positions related to the linear heat generation is shown in Fig. 4-a for both calculation methods (the TEMPIN and FLUENT results are represented by the solid and dashed line respectively). The main temperature discrepancy was observed for the highest values of linear heat generation (which was not relevant for the simulation in the NESTLE code, since these values will never be achieved during coupled simulation and the melting of the fuel and cladding occurs at the corresponding temperatures). The results of fuel maximal temperature and fuel average temperature were consistent for both calculation methods when the linear heat generation of the system was lower than 440 $W.cm^{-1}$. However, the fuel surface temperature deviation was approximately 100 °C for the heat generation 350 $W.cm^{-1}$ (60 °C for the heat generation 200 $W.cm^{-1}$). This behavior was expected due to different modeling procedure of the helium gap. In the FLUENT simulation, the He gap is defined as a static parameter, where the thermal expansion of cladding and fuel is not considered (also Knudsen's permeability correction was not taken into account). Besides, the TEMPIN code took into account also thermal expansion of cladding and fuel. The other approximation results presented in Fig. 4-b and Fig. 5 are formatted in imperial units and the reason for this formatting option is to keep the same unit system as the NESTLE requires for the input. The effective heat transfer coefficient shown in Fig. 4-b was consistent for both calculation methods for the temperatures below 3 100 °F (1 704 °C). This also applies for the approximation of the average fuel temperature related with linear heat generation shown in Fig. 5-a. As expected, the main deviation was observed for the surface temperature approximation due to the different modeling approaches of He gap.

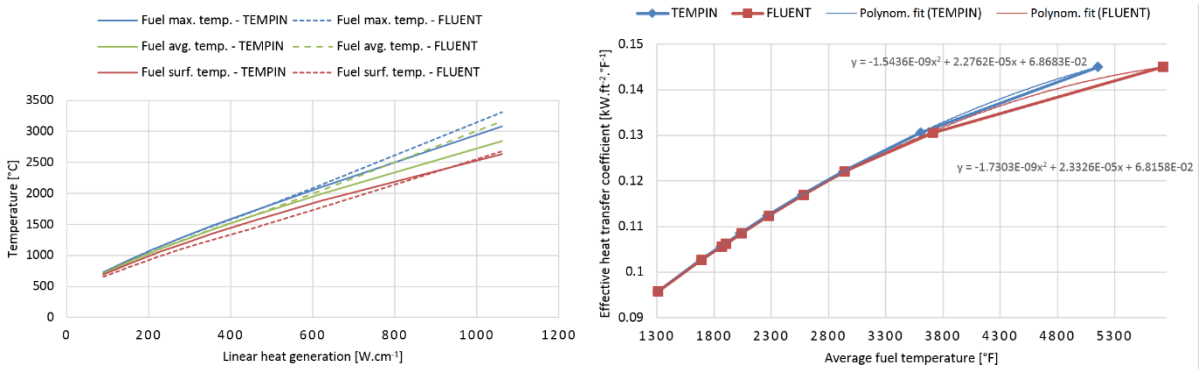

a) Fuel temperature distributions b) Effective heat transfer coefficient

Figure 4: Comparison of fuel temperature distribution and effective heat transfer coefficient for both calculation methods

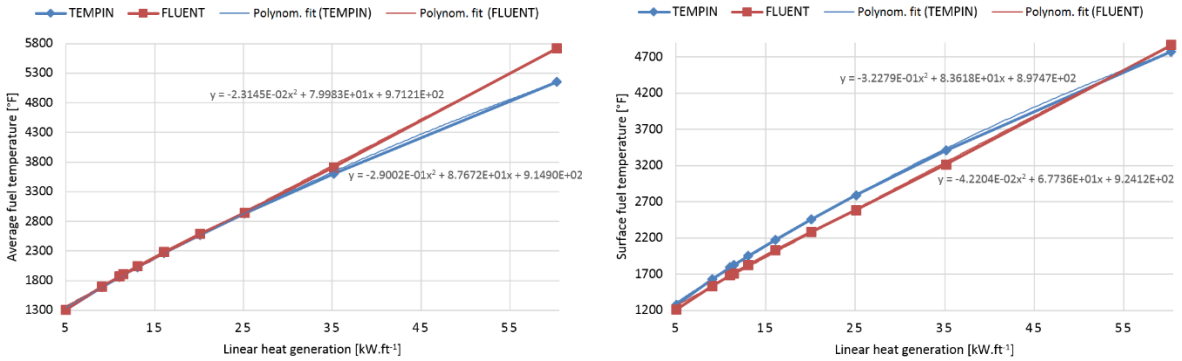

a) Average fuel temperature b) Surface fuel temperature

Figure 5: Comparison of average and surface fuel temperature approximations related with linear heat generation

Based on the prepared thermal-hydraulic approximations, the steady and transient state was simulated by the NESTLE code. The results of the axial temperature distributions for hot channel are presented in Fig. 6 for the steady state calculation. No major differences were observed for this simulation. In the case of the NESTLE simulation with the TEMPIN thermal-hydraulic model (designated as TEMPIN in the figure), the fuel temperatures were slightly lower than temperatures achieved by the FLUENT calculation path (designated as FLUENT). The results of the transient simulation are similarly compared in Fig. 7 and the maximal fuel temperature was achieved within 3.0 s time of the simulation. The discrepancy of the fuel temperatures increased a little bit between the simulation methods. However, this change did not affect the transient state simulation and the actuation time of all NT assemblies was similar for both calculation methods. The NT assembly actuation order and power distributions are shown in Fig. 8. Details about this transient scenario can be found also in [6].

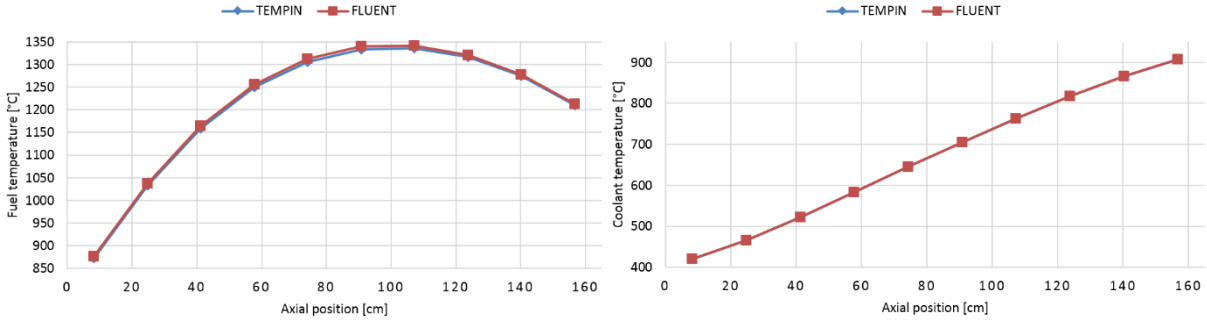

a) Nodal average fuel temperature b) Nodal average coolant temperature

Figure 6: NESTLE results of the hot channel during the steady state simulation

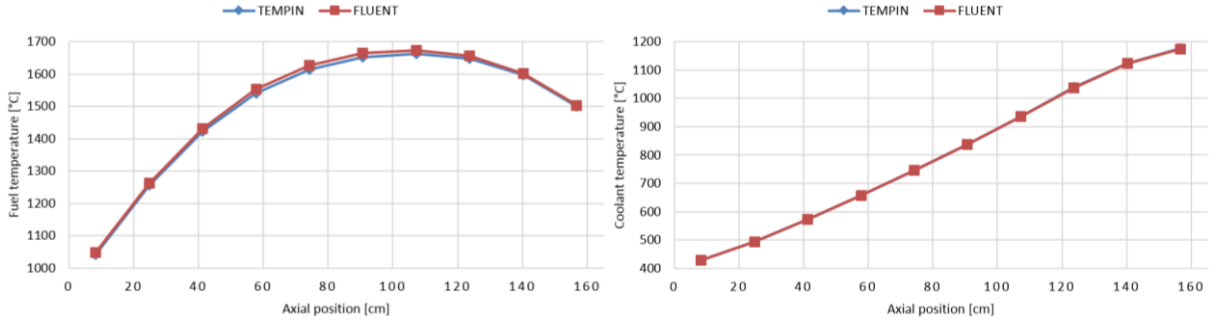

a) Nodal average fuel temperature b) Nodal average coolant temperature

Figure 7: NESTLE results of the hot channel during the transient state simulation

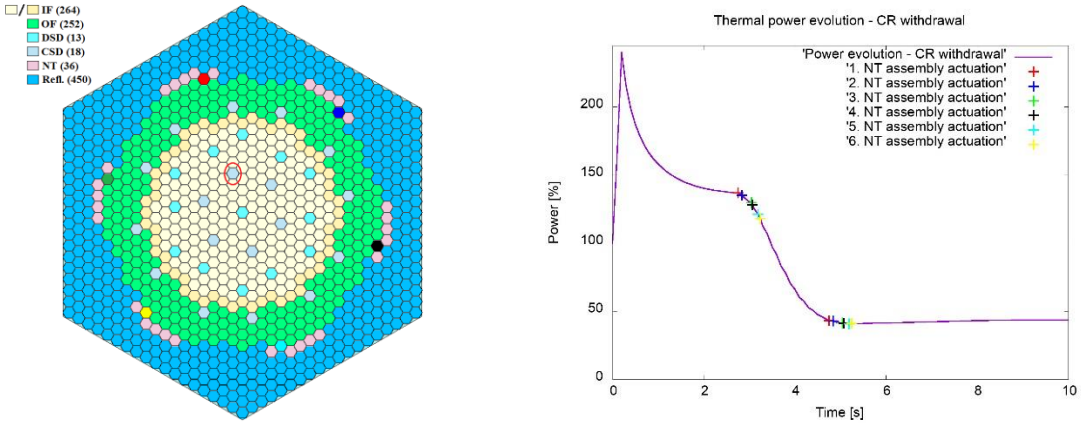

a) NT actuated assemblies b) Power distribution

Figure 8: NT assemblies actuation order and the power distribution during transient scenario

Next application of the TEMPIN code was to determine maximal fuel temperature within the fuel pin. The maximal power peaking factor during whole transient process was estimated on the level 1.781 with corresponding coolant temperature 659 °C in the similar node. Both these values were updated in the TEMPIN calculation to obtain radial temperature distribution of the pin for this region (see Fig. 9). This value of the power peaking factor was achieved only in small time interval during the transient simulation. Therefore, the radial temperature distribution in Fig. 9 can be considered as conservative due to the fact, that distribution was obtained by the steady state simulation in the TEMPIN code. The maximal achieved temperature was 1 842 °C what is less than the melting temperature of the fuel or construction materials within the core.

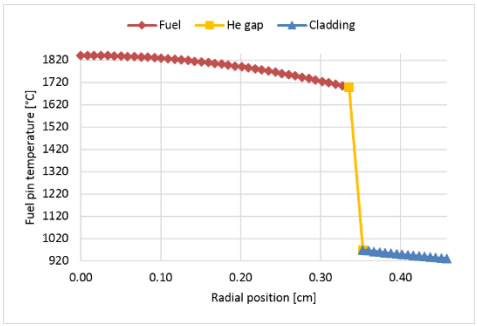

Figure 9: Radial temperature distribution of the fuel pin

5 CONCLUSION

The processing of the thermal-hydraulic approximations is the key element for the performance of the coupled nodal simulator such as NESTLE. Two methods how to obtain suitable approximations for the NESTLE code were presented in the paper. The necessary thermal-hydraulic parameters were processed by the in-house developed code referred as TEMPIN. The results of the TEMPIN code were compared with the FLUENT CFD code and both results were consistent when the linear heat generation of the system was lower than 440 $W.cm^{-1}$. The main discrepancy was observed in the case of the fuel surface temperature distribution and this result was expected due to the different treatment of the thermal-hydraulic properties of the helium gap in the pin. However, this deviation did not influence the NESTLE code simulation significantly and the results of the transient and steady state simulations were almost identical. The next result obtained from the TEMPIN code was the radial temperature distribution within the fuel pin for maximal obtained power generation during the transient simulation. The maximal achieved temperature of the fuel was conservatively determined to 1842 °C what is below the melting point temperature of the fuel and construction materials within the core. The main advantage of TEMPIN is fast computational time (one calculation lasted less than 15 seconds for one power level) and therefore this code can be very suitable for the design calculations of new nuclear power systems.

ACKNOWLEDGMENTS

This study has been partially supported by the Slovak Research Development Agency No. APVV-16-0288 and DS-FR-19-0014, by the Scientific Grant Agency of the Ministry of Education of Slovak Republic and the Slovak Academy of Sciences No. VEGA 1/0863/17 and by the Cultural and Educational Grant Agency of the Ministry of Education of Slovak Republic No. KEGA 041STU-4/2019.

REFERENCES

[1] North Carolina State University (Electric Power Research Center), NESTLE Version 5.2.1 (Few-Group Neutron Diffusion Equation Solver Utilizing the Nodal Expansion Method for Eigenvalue, Adjoint, Fixed-Source Steady-State and Transient Problems), 2003, NC 27695-7909, p. 177.

[2] T. Downar, D. Lee, Y. Xu, T. Kozlowski, PARCS v2.6 U.S. NRC Core Neutronics Simulator - Theory Manual, RES / U.S. NRC, Rockville, 2004.

[3] M. Vitkova, B. Kalchev, S. Stefanova "Regulatory requirements to the thermal-hydraulic and thermal-mechanical computer codes", Proc. International conference on WWER fuel performance, modelling and experimental support, Albena, Bulgaria, 2006, p. 12.

[4] Oak Ridge National Laboratory, SCALE Code System (version 6.2.3), 2018 (ORNL/TM-2005/39), p. 2760.

[5] B. J. Ade, SCALE/TRITON Primer: A Primer for Light Water Reactor Lattice Physics Calculation, 2012, ORNL/TM-2011/21 (NUREG/CR-7041), United States Nuclear Regulatory Commission: Oak Ridge, USA, p. 279.

[6] F. Osuský, B. Vrban, J. Haščík, "Implementation of Neutron Trap Passive System in GFR 2400 Fast Reactor Design", NENE 2019 Proc. 28th Int. Conf. Nuclear Energy for New Europe, Portorož, Slovenia, September 9-12, 2019., p. 8.

[7] F. Osuský, Neutronic study of fast reactor cores with a focus on transient processes (dissertation thesis), STU, Bratislava, 2019, p. 195.

[8] ANSYS, Inc., ANSYS: Fluent Theory Guide, Release 19.1., Help System, 2019.

[9] F. Osuský, B. Vrban, J. Lüley, Š. Čerba, J. Haščík, "Definition of the thermal-hydraulic model of the gas-cooled fast reactor", Journal of nuclear research and development, 15, 2018, pp. 14-18.

[10] Z. Perkó, S. Pelloni, K. Mikityuk, et al., "Core neutronics characterization of the GFR2400 Gas Cooled Fast Reactor", Progress in Nuclear Energy, 83, 2015, pp. 460-481.

[11] Z. Perkó, Sensitivity and Uncertainty Analysis of Coupled Reactor Physics Problems (dissertation thesis), Delft University of Technology, Delft, 2015, p. 219.

[12] V. Verma, A. K. Ghosh, " Thermal Analysis of Metallic Fuel for Future FBRs", Energy Procedia, 7, 2011, pp. 234-249.

[13] B. Vrban, Š. Čerba, J. Lüley, F. Osuský, V. Nečas, "On the effective fuel temperature of VVER-440 fuels", NUPP 2018 Proc. 2nd International conference on nuclear power plants: Structures, risk and decommissioning, London, UK, June 11-12, 2018., pp. 147-155.

[14] R. V. Smith, "Review of Heat Transfer to Helium I*", Cryogenics, 9, 1969, pp. 11-19.